Self-consistent calculations of the strength function and radiative neutron capture cross section for stable and unstable tin isotopes

A. Avdeenkov
National Institute for Theoretical Physics (NIThePP), Stellenbosch 7600, South Africa and Institute of Theoretical Physics, University of Stellenbosch, Stellenbosch 7600, South Africa and Skobeltsyn Institute of Nuclear Physics, Moscow State University, Leninskie gory, Moscow, RU-119991, Russia

S. Goriely
Institut d'Astronomie et d'Astrophysique, ULB, CP 226, B-1050 Brussels, Belgium

S. Kamerdzhiev
Institute of Physics and Power Engineering, RU-249033 Obninsk, Russia and Institut für Kernphysik, Forschungszentrum Jülich, D-52425 Jülich, Germany

S. Krewald
Institut für Kernphysik, Forschungszentrum Jülich, D-52425 Jülich, Germany
(Received 24 March 2011; published 15 June 2011)

The $E1$ strength function for 15 stable and unstable Sn even-even isotopes from $A = 100$ to $A = 176$ are calculated using a self-consistent microscopic theory which, in addition to the standard (quasiparticle) random-phase approximation [(Q)RPA] approach, takes into account phonon coupling and the single-particle continuum (by means of the discretization procedure) with a cutoff of 100 MeV. Our analysis shows two distinct regions for which the integral characteristics of both the giant and pygmy resonances behave rather differently. For neutron-rich nuclei, starting from ^{132}Sn, we obtain a giant $E1$ resonance which significantly deviates from the widely used systematics extrapolated from experimental data in the β-stability valley. We show that the inclusion of phonon coupling is necessary for a proper description of the low-energy pygmy resonances and the corresponding transition densities for $A < 132$ nuclei, while in the $A > 132$ region the influence of phonon coupling is significantly smaller. The radiative neutron capture cross sections leading to the stable ^{124}Sn and unstable ^{132}Sn and ^{150}Sn nuclei are calculated with both the (Q)RPA and the beyond-(Q)RPA strength functions and shown to be sensitive to both the predicted low-lying strength and the phonon-coupling contribution. The comparison with the widely used phenomenological generalized Lorentzian approach shows considerable differences both for the strength function and the radiative neutron capture cross section. In particular, for the neutron-rich ^{150}Sn, the reaction cross section is found to be increased by a factor greater than 20. We conclude that the present approach may provide a complete and coherent description of the γ-ray-strength function for astrophysics applications. In particular, such calculations are highly recommended for a reliable estimate of the electromagnetic properties of exotic nuclei.

DOI: 10.1103/PhysRevC.83.064316 PACS number(s): 24.10.−i, 24.60.Dr, 24.30.Cz, 21.60.Jz

I. INTRODUCTION

One of the paramount and challenging goals of modern nuclear physics is to elaborate theoretical approaches with not only descriptive but also predictive abilities. This is of particular relevance for a proper description of nuclei far from the valley of stability since, in this case, only limited or no information is available. Self-consistency between the mean-field and the effective interaction is also known to be of prime importance for a correct exploration of the excitation properties of unstable nuclei. Another fundamental ingredient of the model, known to be important even for stable nuclei, concerns the inclusion of more complex configurations than those traditionally included in the random-phase approximation (RPA) or quasiparticle RPA (QRPA). Here the most realistic approaches include complex configurations with phonons; namely, the coupling of single-particle degrees of freedom with the phonon degrees (the so-called phonon coupling or PC). These approaches are referred to in the literature as the quasiparticle-phonon model [1], the (Q)RPA + phonon-coupling model [(Q)RPA + PC] [2] and the extended theory of finite Fermi systems (ETFFS) [3]. The latter is based on the Green function method and includes the single-particle continuum which is necessary for nuclei with a nucleon separation energy close to zero. It has been recently generalized to include pairing using the quasiparticle time blocking approximation (QTBA) [4].

These approaches have been supplemented by considering a self-consistent mean field (see, e.g., Ref [5]) or the self-consistency between the mean-field and the effective interaction [6–8]. The latter made it possible to perform the calculation with one unique set of interaction parameters (e.g., the Skyrme force [6,8]) instead of two sets of parameters as used in non-self-consistent approaches (one for the effective interaction and another for the mean field).

These improvements—taking into account the single-particle continuum and self-consistency—are of great interest, first of all, for astrophysics applications, but also for nuclear data evaluation. The added value of such approaches lies essentially in their larger predictive power which provides an increased confidence in the calculation of structure properties for exotic nuclei, especially those with a large neutron excess and/or a small nucleon separation energy. However, one should note that all the approaches developed so far are in fact not fully self-consistent because, as was noted earlier in Refs. [9,10], they use the self-consistency only at the (Q)RPA level and do not include more complex configurations into the self-consistency conditions. This is one of the main reasons to use some additional procedures to exclude ghost states; in particular, the spurious isoscalar 1^- state. This is achieved through a specific fit of the force parameters [5,6,8], the use of the so-called subtraction procedure in the QTBA model [4], or of the so-called forced consistency method [11,12]. Nevertheless, accounting for PC and self-consistency increases, beyond any doubt, the quality of the microscopic nuclear theory and is absolutely necessary to simultaneously describe the structure of ground and excited states for unstable nuclei.

The role played by PC in the description of the giant resonances in stable nuclei is well known. In particular, PC explains approximately 50% of the observed width, its gross structure, and sometimes some fine structure (e.g., for the $E2$ isoscalar resonance in ^{208}Pb [3]). However, the direct influence of PC on the giant resonance of unstable nuclei has been much less studied, although it is expected to be as important as it is for stable nuclei. So far, giant-resonance characteristics for unstable nuclei have been studied systematically within the (Q)RPA only (see, e.g., [13–16]) and, quite recently, within a general approach based on sum rules [17]. Note that, for the reasons given below, we will discuss in the present paper only the case of electric dipole resonance.

The impact of PC on the so-called pygmy dipole resonance (PDR), which lies in the low-energy tail of the $E1$ giant dipole resonance (GDR) and exhausts about 1%–2% of the energy-weighted sum rule (EWSR) [14,18–20], is of particular interest. First, there is no consensus at present in our understanding of some important questions related to the PDR (see Ref. [13] and the recent reviews [21,22]). Second, this resonance is known to have a significant impact on the radiative neutron capture rate of astrophysical interest [14,15,23]. The importance of the PDR is confirmed by the simple fact that it has been taken into account in all modern nuclear data libraries (although at a phenomenological level) in addition to the usual GDR [20,24]. The question arises for exotic nuclei where the phenomenological approach may fail to provide a reliable prediction because of the specific features of the PDR in such nuclei and the scarce experimental data on which systematics is based. For this reason, a similar approach should be followed as for the giant resonance problem for unstable nuclei; namely, as discussed above, to use a reliable self-consistent theory which accounts for PC and the single-particle continuum in addition to the standard (Q)RPA.

For all these reasons, the PDR problem has recently become a subject of intensive experimental (see Refs. [18,19,25] and references therein) and theoretical (see Refs. [5–7,21,26–28] and references therein) studies. Even if the total $E1$ strength of the PDR is small, if it is located well below the neutron separation energy, it can significantly increase the radiative neutron capture cross section, especially for neutron-rich nuclei [14,15,23]. Different measurements suggest that some enhancement of the $E1$ strength could be located at low energies even in stable nuclei, a feature that cannot be described within the (Q)RPA calculations. In particular, the large-scale QRPA calculations of [14] predict PDRs which are, on average, 1 to 2 MeV higher in energy than the observed values. Many recent calculations of the PDR [6,7,21,28–30] as well as the older ones [31,32] performed within the non-self-consistent quasiparticle-phonon model confirm the need to take into account more complex configurations than those included in the (Q)RPA approach, most of all the 1p1h $\otimes$ phonon or 2 quasiparticle $\otimes$ phonon configurations. However, large uncertainties in the description of the PDR (in particular, its energy and strength) remain, especially for unstable nuclei, and only sound microscopic models can shed light on its existence, as well as its relative importance and impact on neutron capture. For example, self-consistent calculations with PC [28,33] have shown that the complex configurations give a significant contribution to the radiative neutron capture cross section for the unstable ^{132}Sn.

In practice, for a proper description of the PDR, at least two natural physical conditions need to be fulfilled: first, the energy of the 1^- spurious state must be equal to zero; second, the theory must describe correctly the mean energy E_0 of the $E1$ giant resonance. Only in this case may one expect the theory to provide a reasonable quantitative prediction of the PDR integral features. In order to satisfy these two conditions, different additional procedures have been used. The simplest way is to adjust the isovector and isoscalar effective force parameters to obtain the correct values of E_0 and the spurious 1^- level energy [5]. This is suitable for stable nuclei for which E_0 is experimentally available. For unstable nuclei, if use is made of a Skyrme force and a self-consistent scheme without the subtraction procedure [4], it is necessary to modify some of the Skyrme parameters to obtain agreement with experiment [8,34]. It is worth noting that this conclusion is in accordance with the studies of Refs. [35,36] who considered this idea from a different point of view.

In our previous works [8,21,28] we realized a self-consistent version of the ETFFS(QTBA) using a discretized single-particle continuum with different kinds of Skyrme forces including the SLy4 forces, where the velocity force is considered in a local approximation (sometimes we call it DTBA). The latter had consequences for the renormalization of the interaction in order to locate the spurious state at zero energy. On the one hand, it is of great interest to obtain general information about the $E1$ strength function and correspondingly about the radiative neutron capture cross section for many neutron-rich nuclei using the well-known SLy4 forces. On the other hand, it is clear that the inclusion of the single-particle continuum along with PC effects for nonmagic nuclei is still a difficult problem. For these reasons,

we use here our DTBA approach to calculate the $E1$ strength function for the long Sn isotopic chain.

The aim of the present work is twofold. First, we calculate the PDR and GDR in the long chain of stable and unstable tin isotopes using the variant of the microscopic self-consistent version of the ETFFS(QTBA) which, in addition to the (Q)RPA approach, takes into account the single-particle continuum (by means of the discretization procedure) and phonon coupling in nuclei with pairing. For this part we concentrate on the description of the integral characteristics in order to gain an insight into different trends for stable and unstable nuclei and to compare our results with the widely used empirical formula. Second, in order to investigate the impact of PC on the radiative neutron capture cross section in stable and unstable nuclei we calculate them both with and without PC, within the same scheme of calculation based on the SLy4 Skyrme force or a slightly modified version of it. Here our main focus is on the PDR and its impact on radiative neutron capture.

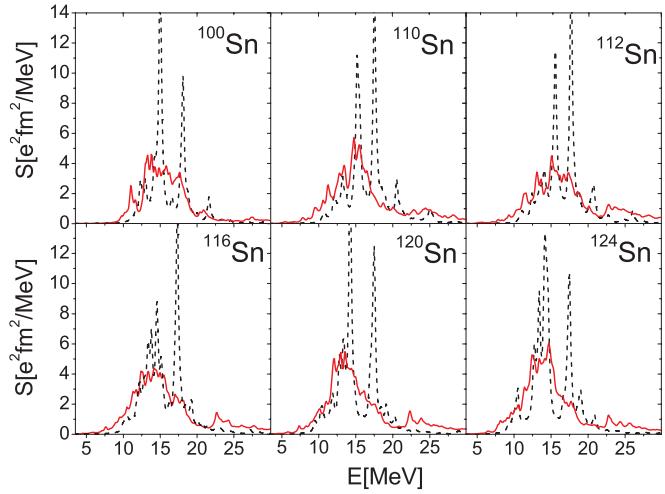

FIG. 1. (Color online) 1^- strength functions within QRPA (dashed curves) and QTBA (solid curves) for ^{100}Sn,^{110}Sn,^{112}Sn,^{116}Sn, ^{120}Sn, and ^{124}Sn isotopes.

II. SELF-CONSISTENT CALCULATION OF THE PDR AND GDR

A. Method

To date there are tens of different Skyrme parametrizations serving slightly different aims and fitting some bulk properties of the ground state. Here we use the SLy4 parametrization of the Skyrme force [37], which proves to be rather successful in describing bulk properties of the ground state and some excited states within the (Q)RPA [38].

The ground states are calculated within the Hartree-Fock-Bogoliubov (HFB) approach using the spherical code HFBRAD [39]. The residual interaction for the (Q)RPA and QTBA calculations is derived as the second derivative of the Skyrme functional [38]. Although the QTBA model [4] was originally formulated in terms of the general basis, several simplifications are performed in our calculations. Namely, the QTBA approach is designed to use the BCS-based quasiparticle basis and we use the HFB approach to extract the quasiparticle characteristics and corresponding wave functions (i.e., the occupation numbers are treated as per the BCS approximation). The spin-orbit residual interaction is dropped. The velocity-dependent terms of the Skyrme force are approximated by their Landau-Migdal limit [40,41], although some more physically sound modifications are included. There are two kinds of velocity-dependent terms: the first one is $\propto \mathbf{k^2}\delta(\mathbf{r}-\mathbf{r}')$ and the second one is $\propto \mathbf{k}^\dagger\delta(\mathbf{r}-\mathbf{r}')\mathbf{k}$ (P-wave interaction in momentum space). The averaged value over the density of the first term gives $k_F^2/2\delta(r-r')$ while that of the second one is zero. Such an approximation violates the self-consistency and one has to correct the parameters of the residual interaction to put the spurious center-of-mass state to zero. We only replace here the term which is proportional to $t_1\mathbf{k_F^2}\delta(\mathbf{r}-\mathbf{r}')$ by a given factor as we take this term approximately. This factor is usually around 1.0–1.25 for the Sn chain.

In general, the ETFFS(QTBA) accounts for the single-particle continuum completely at the RPA level for magic nuclei and includes the new effect of ground-state correlations caused by PC [3]. However, because of the technical difficulties connected with pairing, these effects are not considered in the present calculations. A quasiparticle energy cutoff of 100 MeV is used. We checked that, within this approach, the EWSR is fully exhausted (for the case without the velocity-dependent terms) and that the use of a larger basis did not bring any noticeable differences. The QTBA calculations are performed with the same basis. We use 14–16 low-lying phonons of $L = 2$–6 multipolarity and normal parity. They are obtained within the (Q)RPA with the calculated effective interaction using the same quasiparticle-energy cutoff. Such a consistent method to calculate phonons is the reason we use a larger number of phonons than in the phenomenological ETFFS [3]. In Fig. 1 we test our numerical approximation of the single-particle continuum discretization for the ^{132}Sn and ^{176}Sn magic nuclei by comparing our RPA results with the exact account for the continuum by the Green function method at the RPA level [42,43], as described in Ref. [34]. It turns out that both calculations are almost identical, which confirms that the discretization procedure adopted here is quite satisfactory for GDR at least when a large smearing parameter is used [44]. In the case of the low-lying 1^- strength (PDR) study, one had better use a small smearing parameter in order to identify its more realistic structure. In this case the discretization procedure may not be satisfactory, especially for nuclei with a small nucleon separation energy. Altogether, for small smearing parameters and for nuclei with small separation energy, one should analyze and maybe account for the widths of the single-particle levels in the discrete part of our generalized propagator (see [3]), and we plan to do it in the future. But here we only want to understand the general tendency for the long chain of tin isotopes that results from taking PC into account.

Usually the GDR strength function is obtained from the experimental photoabsorption cross section which is fit by a simple Lorentzian functional. The $E1$ photoabsorption cross section is related to the strength function $S(\omega)$ as follows: $\sigma_{E1}(\omega) = 4.022\,\omega S_{E1}(\omega)$, where the photon energy ω is in MeV, S is in fm^2 MeV^{-1}, and σ is in mb. The Lorentzian fit

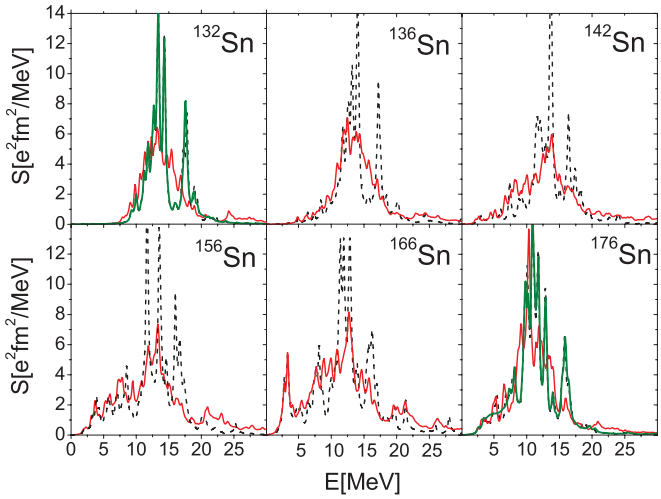

FIG. 2. (Color online) 1^- strength functions within QRPA (dashed curves) and QTBA (solid curves) in ^{132}Sn,^{136}Sn,^{142}Sn,^{156}Sn,^{166}Sn, and ^{176}Sn. For the ^{132}Sn and ^{176}Sn isotopes, the solid green curves show calculations within the continuum RPA.

can be used to estimate the integral characteristics of the giant resonance [45,46]. The mean energy E_0, the resonance width Γ, and the maximum value of the cross section σ_0 are extracted from the calculated photoabsorption cross sections under the condition that the three lowest energy-weighted moments of the Lorentzian and of the theoretical curve should coincide in the energy interval considered. However, in order to obtain more complete and universal information about the integral characteristics, it is often better to use energy moments (see below). This seems to be more appropriate for very neutron-rich nuclei where one may expect significant deviations from a Lorentzian-like shape for the cross section. The same (0–30) MeV summation interval is used for all considered nuclei.

The other feature of our calculation scheme is the so-called subtraction procedure [4,7] which should avoid a PC double counting from the effective interaction. This procedure is a direct continuation of the phenomenological refinement philosophy used in the first formulations of the ETFFS [3,47]. Because the self-consistent relativistic (Q)RPA calculations fit the experimental data well and because the subtraction procedure, in principle, provides the correct E_0 value, which is equal to the (Q)RPA E_0 value, the authors [7] obtained a fulfillment of the above-mentioned conditions if the energy interval is properly chosen, for example (10–22.5) MeV for $Z = 50$ nuclei or (10–25) MeV for $N = 50$ nuclei. However, together with a reasonable description of the GDR's width, PC gives an additional strength in the low-energy region (see Figs. 1 and 2). So this low-energy contribution of the strength is usually neglected in such an analysis of the integral characteristics based on the Lorentzian fit.

B. Results

Here we discuss our results for the long chain of tin isotopes from ^{100}Sn up to ^{176}Sn. Figures 1 and 2 show the strength functions for twelve Sn isotopes. In the following subsections, the dipole excitations are studied and the GDR and PDR analyzed along the Sn isotopic chain. The general idea behind such an investigation is to understand if there are some common trends for dipole excitations in stable and unstable isotopes on both sides of the β-stability valley and if they can be described within one unique scheme and with one unique force like SLy4. One can argue that such a force may not be appropriate for unstable species but this force is among the most suited tool and can provides us with valuable theoretical findings; for example, as the non-Lorentzian shape of the GDR for very neutron-rich nuclei such as ^{156}Sn and ^{166}Sn (see Fig. 1), as discussed below.

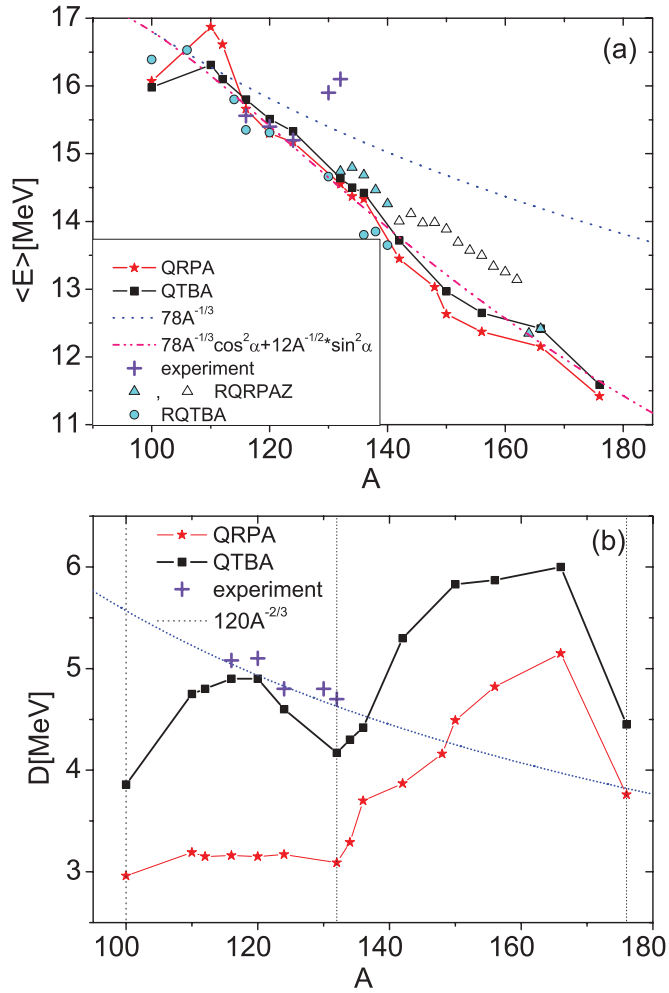

FIG. 3. (Color online) Integral characteristics of the 1^- state for some Sn isotopes. Upper panel: GDR mean energy versus the atomic mass number A in the 0–30 MeV interval. Lower panel: GDR dispersion versus A for the same interval. RQTBA and RQRPAZ results are taken from Refs. [48] and [7], respectively.

1. Dipole excitations and giant dipole resonances

Figure 3 shows the calculated integral characteristics of the dipole excitations for fifteen stable and unstable Sn isotopes. The smearing parameter is $\Delta = 200$ keV for all calculations. The $E1$ response-integral characteristics for the mean energies

and dispersions are calculated using the standard definitions

$$\langle E\rangle = E_{1,0} = \frac{m_1}{m_0}, \quad D = \sqrt{\frac{m_2}{m_0} - \left(\frac{m_1}{m_0}\right)^2}, \tag{1}$$

where the energy moments m_k for the energy interval $\Delta E = E_{\max} - E_{\min}$ are calculated as follows:

$$m_k = \int_{E_{\min}}^{E_{\max}} dE E^k S(E). \tag{2}$$

First we check our approach on the stable Sn isotopes (^{116}Sn, ^{120}Sn, ^{124}Sn) and obtain, as shown in Fig. 3, a reasonable agreement with available experimental data [20]. The dipole excitation for these nuclei has a nicely visible Lorentzian-like form with parameters which may vary slightly depending on the adopted model [20]. Although our results are not fit by a Lorentzian form and only moments are compared, it can be seen that we have a reasonable agreement for both the mean energy and the width of the $E1$ resonance. The ^{132}Sn and ^{130}Sn are the only unstable tin isotopes which were probed to study the GDR and PDR [49]. Although the SLy4 forces works quite well for stable nuclei, there is no proof that it is good for unstable nuclei. In Ref. [8], along with SLy4 Skyrme forces, we probed BSk5 [50] and SkM* [51] for ^{132}Sn. In all the three cases we obtained very similar mean-energy values and widths (i.e., 14.3 and 2.9 MeV, respectively, for the SLy4 force), while the experimental data are 16.1 ± 0.7 and 4.7 ± 2.1 MeV [49]. It has to be noted that other theoretical approaches (see Fig. 3) [7,48] give very similar results, which possibly means that further experimental investigations on the ^{132}Sn GDR may be needed.

Our calculations show a noticeable difference both between (Q)RPA and ETFFS(QTBA) approaches and stable and unstable nuclei (Figs. 2 and 3). The results for integral characteristics (Fig. 3) clearly show the necessity to take PC into account for a proper determination of the GDR width. For the $A = 100$–132 nuclei, PC gives rise to an increase of the width by as much as 2 MeV compared with (Q)RPA predictions. This PC effect is also important in $A > 132$ nuclei, although to a lesser extent. Figure 3 shows two distinct regions for the integral characteristics. The first region corresponds to the stable isotopes, $116 < A < 124$, for which the integral characteristics follow the well-known phenomenological systematics (e.g., $E_0 \propto A^{-1/3}$ and $\Gamma \propto A^{-2/3}$). The second region includes unstable isotopes, $A > 132$, for which these systematics fail. Similar conclusions for mean energies can be made out of the calculations obtained within the relativistic deformed QRPAapproach (RQRPAZ) approach [48].

Here we suggest other empirical systematics which describe quite well the mean energy in both regions defined above:

$$E_0 = 78A^{-1/3}\cos^2\alpha + 12A^{-1/2}\sin^2\alpha, \tag{3}$$

where $\alpha = (N - Z)/A$ is the neutron excess and the factor $12A^{-1/2}$ describes empirically the pairing gap, see Ref. [52]. One can see that this is in accordance with the results in Fig. 6 (see below). The first term is responsible for the collective GDR while the second one reflects the leftovers of the GDR; namely, the noncollective particle-hole excitations. This formula reflects the fact that the mean energy depends on the superposition of these two kinds of excitations, while the degree of mixing is defined by the neutron excess α. The second term becomes important for unstable nuclei and is correlated with the increased low-lying $E1$ strength. As mentioned above, the $E1$ strength can hardly be described by a Lorentzian function over the whole isotopic chain. One may also try to separate out the GDR and PDR in the same way as done in Ref. [48] using ^{132}Sn as the benchmark in the definition of the border between these two resonances. This procedure is somewhat artificial and, anyway, for unstable nuclei the GDR centroid energy itself does not follow the systematics, nor does the mean energy taken in the whole 0–30 MeV interval. Another interesting feature is that the dispersion (Fig. 3, lower panel) is minimal at neutron magic numbers ($N = 50$, 82, 126) and maximal for open shell nuclei. Likewise for the mean energy, the dispersion is quite close to the Lorentzian width for stable nuclei only, while the contribution of the low-lying tail to the dispersion for the second region is increasingly important with increasing neutron excess.

2. *Pygmy dipole resonances*

The division of the dipole excitation between the GDR and PDR regions seems rather artificial, although the nature of the vibrations is rather different: the low-energy neutron and proton transitional densities are vibrating mainly in phase, while in the GDR energy region these are out of phase (see, for example, the case of ^{208}Pb in Ref. [53]). But there is no general rule for defining the interval of pygmy dipole excitations for a given nucleus. We can only visually outline the transition region between the GDR and PDR. We find that, for the whole Sn chain, this region is rather well described by the 8 to 10 MeV interval, as illustrated in Fig. 4.

This is why we consider here the 0–10 MeV interval for all the nuclei—to get a general understanding about the low-lying dipole strength. The resulting mean energies $\langle E\rangle = E_{1,0}$ and $\Sigma B(E1)$ values are shown in Fig. 5, along with the relativistic QTBA (RQTBA) [7,54] and RQRPAZ [48] results as well as the available experimental data [32,55].

We compare our results with these two relativistic approaches because they are the only available calculations of integral characteristics for both the GDR and PDR in many isotopes of the Sn chain and they have been obtained within a self-consistent scheme. It has to be noted that experimental data is available for ^{112}Sn, ^{116}Sn, and ^{124}Sn isotopes up to the neutron separation energy (the low-lying strength is mostly concentrated in the 4–8.5 MeV interval) while the "pygmy region" for ^{130}Sn and ^{132}Sn isotopes is not indicated in Ref. [55].

We obtain a reasonable agreement with experiment for the $\langle E\rangle$ values summed over the 4–8.5 MeV interval (Fig. 5) while the integral strength is a few times larger than the experimental value. A similar behavior was observed in other self-consistent calculations [48] (see Fig. 5). We find some sort of agreement with the experimental ^{132}Sn data (for our 0–10 MeV interval), which gives an integrated strength of the PDR of about $4\% \pm 3\%$ of the EWSR [57], while our calculation gives 4% with PC included and 2% without. At the same

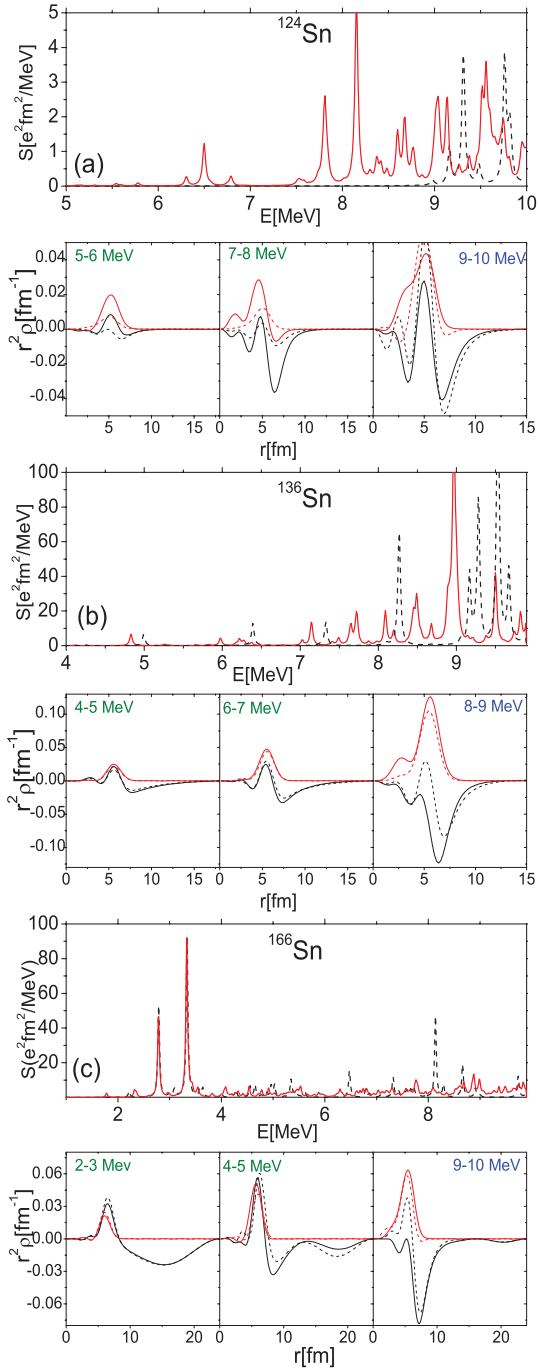

FIG. 4. (Color online) For each of the stable ^{124}Sn and unstable ^{136}Sn and ^{166}Sn, the upper panel shows the strength function obtained within QRPA (dashed curves) and QTBA (solid curves) in the 0–10 MeV interval and the lower panel shows the corresponding transitional densities for protons (red curves) and neutrons (black curves) summed over the indicated intervals. The smearing parameter is 20 keV.

time the calculated and experimental GDR mean energies are rather different and, moreover, the experimental mean energy is out of the general trend (Fig. 3). Out of our self-consistent calculations for the Sn chain and other non-self-consistent calculations as in Ref. [5], we conclude that the PDR is very

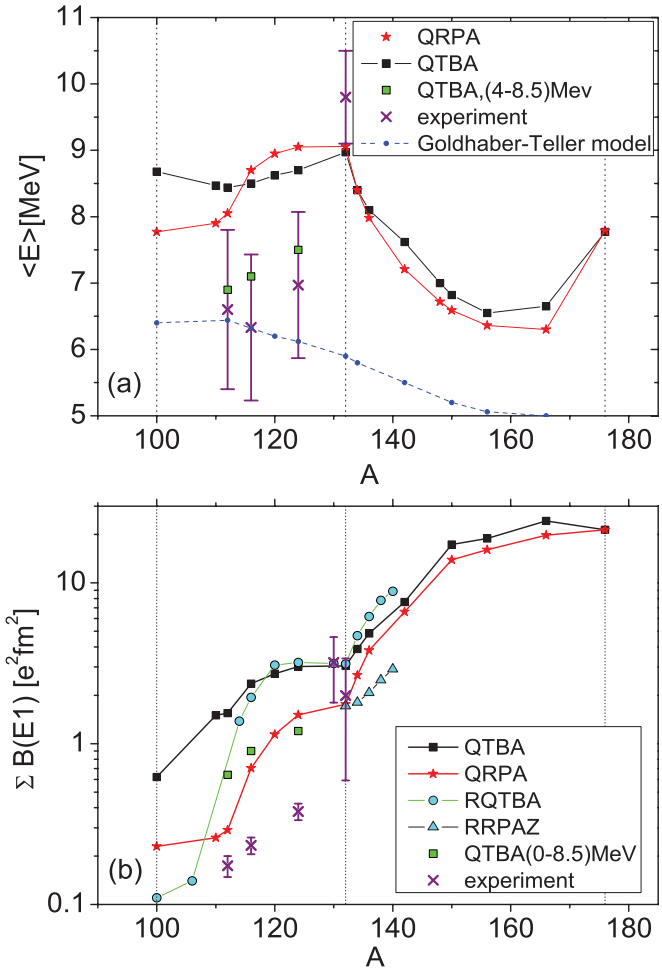

FIG. 5. (Color online) Integral characteristics of 1^- states in the 0–10 MeV interval. (a) Mean energy versus the atomic mass number A. (b) $\Sigma B(E1)$ values. RQTBA and RQRPAZ results are taken from Ref. [48] and [54], respectively. The results for Goldhaber-Teller model are based on the work in Ref. [56]. Experimental results for $\langle E\rangle$ and $\Sigma B(E1)$ are taken from Refs. [32] and [55], respectively.

model-dependent and the force adopted probably needs some modifications for a simultaneous description of both the GDR and PDR. It is also rather evident that further experimental investigations are needed as well.

Figures 4 and 5 demonstrate that there is a distinct difference for characteristics of a low-lying strength for stable and unstable nuclei; namely, the PC contribution to $\Sigma B(E1)$ (i.e., the difference between the QRPA and QTBA predictions) is small for nuclei in the $A > 132$ region, while in the $A < 132$ region PC has a rather important impact. Moreover, for nuclei such as ^{112}Sn, ^{116}Sn, and ^{124}Sn (Fig. 4, upper panel) the PDR is almost completely defined by complex configurations in the 4–8.5 MeV interval. For the $\langle E\rangle$ values we also have a "border" at $A = 132$. In the $A > 132$ region there is almost no PC contribution and a decrease of $\langle E\rangle$, while in the $A < 132$ region this picture is more complicated: the PC contribution "corrects" an A dependence of the $\langle E\rangle$ values, which would be expected within the QRPA approach, and in this sense the PC effect is important.

We find that the structure of the PDR excitation spectrum is very specific to each nucleus. It is hardly a collective mode and cannot be described by some systematics like the GDR. For example, the Goldhaber-Teller model adapted for neutron-rich nuclei in Ref. [56] gives a rather smooth A-dependent behavior for the PDR mean energy and its strength (Fig. 5), which is not predicted by our calculations and which is not really confirmed by available experimental data. This is easy to understand from the simple Brown-Bolsterly model for the (Q)RPA approach. Indeed, in this model the excitation properties are determined by the structure of single-particle or single-quasiparticle levels; namely, the larger the difference between the neighboring levels, the more collective the appropriate (Q)RPA 1^- level. From this point of view, the collectivity is determined by the structure of single-(quasi)particle levels and, therefore, the PDR structure is rather specific to each nucleus. Moreover, recently a thorough theoretical analysis on the PDR collectivity in ^{132}Sn was performed in Refs. [58,59], which shows that the collectivity is rather weak and only a few particle-hole configurations contribute to the PDR. The authors demonstrated that such contributions are force-dependent and cooperative but not coherent.

In order to better understand the PC role in the PDR region for stable and unstable nuclei it is useful to consider the correlation between the neutron separation energy and the beginning of the low-energy excitation spectrum. In Fig. 6, we compare the neutron separation energy with the minimal particle-hole energy $(E_p + E_h)$ and the minimal energy $(E_p + E_h + \omega)$, where ω is the energy of the lowest phonon for a given isotope, which approximately determine the "beginning" of the low-lying tail for the (Q)RPA and QTBA models, respectively. We see clearly that, the smaller the neutron separation energy is, the lower is the energy of the first 1^- level. One can see also a border at $A = 132$; that is, a direct correlation and similarity in the beginning of the spectrum within both the (Q)RPA and QTBA for the neutron-rich isotopes.

Due to the small neutron separation energy in the very neutron-rich Sn isotopes, a relatively strong low-lying tail of the strength function arises very naturally both within the QRPA and QTBA (see Figs. 1 and 4). So, there is no noticeable difference here between these two approaches. In contrast, for the lighter Sn isotopes (see Figs. 2 and 4), a considerable contribution of PC can be observed.

To conclude our analysis of the PDR, we consider transition densities which are now a standard way to investigate the nature of nuclear excitations. Recently, this analysis was performed for some tin isotopes within the QRPA approach [5,58,60] and within the relativistic QTBA [54]. In Fig. 4, we show our self-consistent QRPA and QTBA results for the stable ^{124}Sn isotope and the unstable ^{136}Sn and ^{166}Sn isotopes. We obtain a rather similar behavior for ^{136}Sn and ^{166}Sn isotopes within the QRPA and QTBA approaches: below 8 MeV (^{136}Sn) and 9 MeV (^{166}Sn) the proton and neutron transition densities are in phase in both approaches; that is, both have an isoscalar character and are clearly dominated by the neutron contribution at the surface. At higher energies they show an isovector behavior. Globally, our results are in accordance with the QRPA results of [5,60] for stable nuclei. However, we would like to emphasize some major differences between the QRPA and QTBA approaches as far as the transition densities for the stable ^{124}Sn isotope are concerned (Fig. 4). Physically, this corresponds to the fact that the PC gives a considerable contribution to the low-lying strength in stable nuclei, which can clearly be seen in Figs. 2 and 4 for other stable nuclei.

In summary, we find that with the inclusion of PC the low-lying tail is predominantly of isoscalar nature up to about 8 MeV for all considered Sn isotopes while the ≈8–10 MeV interval is a transition region toward the isovector-type of excitation which distinguishes the GDR. We also conclude that the inclusion of PC is necessary to explain the PDR integral properties (including the integrated strength) in stable isotopes. Moreover it is mostly PC that contributes below the neutron separation energy. For the $A > 132$ nuclei, and especially for unstable neutron-rich nuclei, PC leads essentially to a redistribution of the PDR strength.

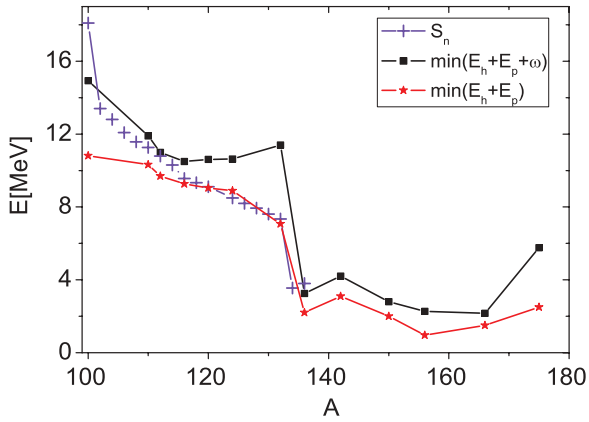

FIG. 6. (Color online) Comparison of the neutron separation energy with the minimal particle-hole energy $(E_p + E_h)$ and the minimal energy $(E_p + E_h + \omega)$, where ω is the energy of the lowest phonon for the different Sn isotopes. See text for more details.

III. RADIATIVE NEUTRON CAPTURE CROSS SECTIONS

The presence of the PDR in neutron-rich nuclei is of particular interest since, if located well below the neutron separation energy, it can significantly increase the radiative neutron capture cross section and affect the nucleosynthesis of neutron-rich nuclei by the so-called r process [14,15,23,61]. Similarly, the presence of extra strength at low energy in neutron-deficient nuclei can be at the origin of an increase of the radiative proton capture or photoproton emission that takes place on the left side of the β-stability valley during the so-called rp process or p process, respectively [62]. Since such nucleosynthesis processes involve exotic nuclei that cannot be produced in the laboratory (at least on the neutron-rich side), only self-consistent calculations can provide a reasonable prediction of their electromagnetic excitation properties. The impact of our newly derived strength functions on the reaction cross section are discussed below.

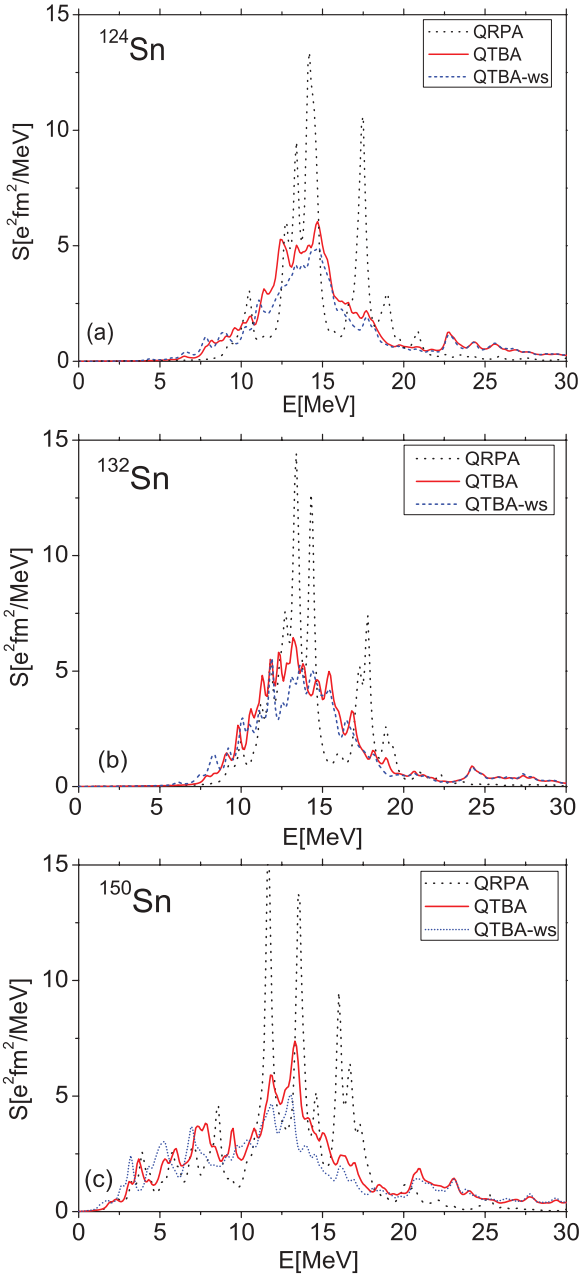

FIG. 7. (Color online) 1^- strength functions within QRPA (dotted curves), QTBA (solid curves) and QTBA-ws (short-dashed curves) for ^{124}Sn,^{132}Sn and ^{150}Sn isotopes. See text for details.

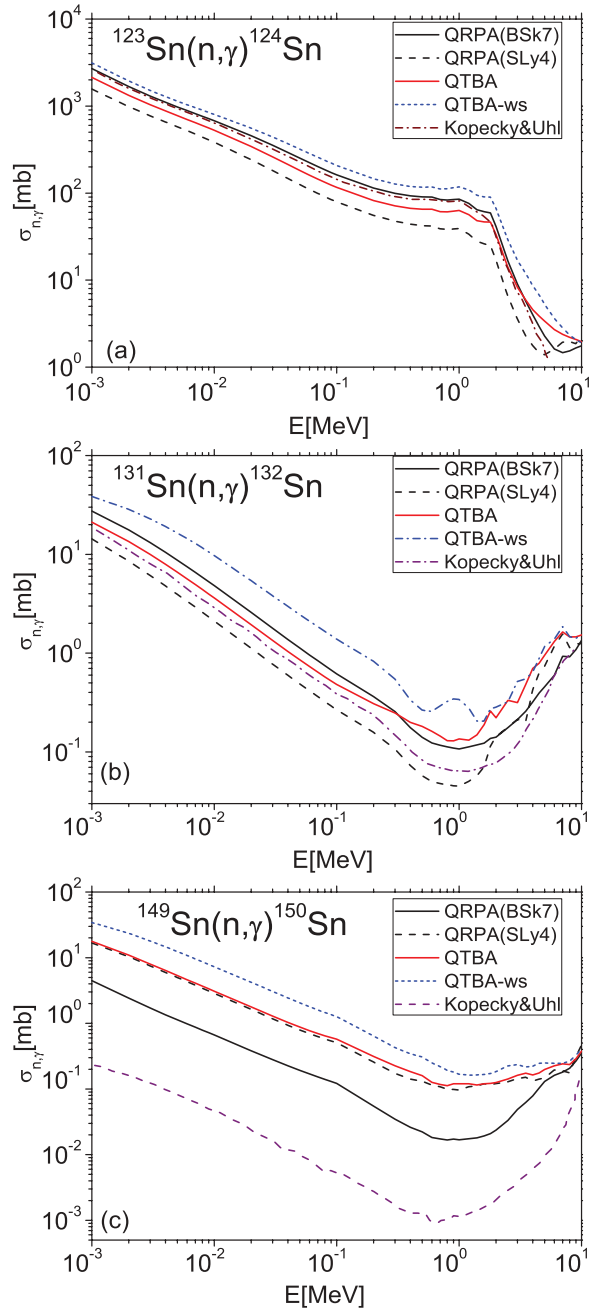

FIG. 8. (Color online) Radiative neutron capture cross sections for ^{124}Sn, ^{132}Sn, and ^{150}Sn isotopes obtained with the strength functions which were calculated within the QRPA, QTBA, and Kopecky-Uhl approaches. See text for details.

A. Comparison between QTBA and QRPA

To estimate the impact that our new QTBA strength can have on the radiative neutron capture rate of astrophysical interest, the neutron capture cross section is calculated using the reaction code TALYS [63]. The strength function with and without PC is included in the calculation of the electromagnetic deexcitation transmission coefficients. The resulting radiative neutron capture cross sections calculated with the strength functions of Fig. 7 are shown in Fig. 8 for the three Sn isotopes.

In Ref. [28], we studied the ^{143}Nd(n, γ)^{144}Nd cross section using the non-self-consistent ETTFS(QTBA) strength function. Comparison with the QRPA version showed that PC inclusion increases the cross section by a factor of two and improves the agreement with experiment [64]. Very recently, the results of calculations of the radiative neutron capture cross sections within the self-consistent relativistic QTBA were performed for the four tin isotopes [65].

Since the electromagnetic transmission coefficient corresponds to an integral overlap of the deexcitation strength function with the nuclear level density, only the strength function in a restricted energy range below the neutron separation energy plays an important role for the estimate of the

radiative neutron capture rate [61,66]. This range corresponds to γ energies typically in the range of 2 MeV $< E_\gamma <$ 4 MeV, although it may be higher in neutron-deficient nuclei or just before crossing a neutron closed shell. Therefore, if located in this energy range, the PDR might provide quite a large contribution to the radiative cross section. For neutron-rich nuclei, the mean PDR energy is relatively low and the integrated strength is high (Fig. 5), so that the PDR contribution may become significant [14,15].

Here we consider three different compound Sn nuclei; namely, the stable ^{124}Sn isotope and the unstable ^{132}Sn and ^{150}Sn isotopes. In our earlier calculations [28,67] we used the microscopically calculated (Q)RPA and QTBA strength functions, which were folded with a Lorentzian, in order to reproduce the expected width of the strength function. However, such a procedure tends to smear out the detailed structure of the strength function that may be of interest in the specific energy of relevance (as discussed above). For this reason, we consider here the realistic strength functions without any Lorentzian folding.

We consider two variants of the QTBA calculations in order to compare the ETFFS(QTBA) calculations with and without (QTBA-ws) the subtraction procedure (see the end of Sec. II A). In the variant QTBA-ws, the isovector part of the calculated effective interaction strength [8] is renormalized in order to bring (in this approach) the mean energy E_0 Eq. (1) to the QTBA-predicted value; that is, to fulfill the condition E_0(QTBA) $= E_0$(QTBA-ws). It turns out that the change of the isovector part is no more than 10% (more precisely 8%, 5%, and 10% for ^{124}Sn, ^{132}Sn, and ^{150}Sn, respectively). We find that the difference between the QTBA and QTBA-ws strength functions is not large; both of them differ significantly from the QRPA predictions (see Fig. 7). The differences between QTBA and QTBA-ws are essentially found in the redistribution of the strength. This effect, however, is large enough to impact the radiative neutron capture cross section, as shown in Fig. 8.

In particular, Fig. 8 shows that the QTBA-ws gives a larger cross section compared with the QTBA for all the three isotopes, although the GDR mean energies are the same for both variants. The comparison with the corresponding RQTBA calculations for ^{131}Sn$(n, \gamma)^{132}$Sn cross section [65] shows, in general, similar behavior, except for specific energies like those around $E_n = 100$ keV for which our cross section is noticeably smaller than the RQTBA one. These deviations may stem from the specific structure of the strength function in the energy range of relevance, as well as from the use of different nuclear ingredients in the cross-section calculation, such as nuclear level densities.

In Refs. [28,67], where the microscopic strength function is folded with a Lorentzian function, we found that, for the stable ^{124}Sn, the cross sections obtained with QRPA and QTBA were almost identical. Comparing the QTBA and QRPA strength functions (Fig. 7) and cross sections (Fig. 8) allows us to deduce directly the role of PC (without any interference of an additional Lorentzian smoothing). In particular, the inclusion of PC increases the cross sections by a factor two to three in the QTBA-ws case (Fig. 8). In the latter case, the cross section obviously follows the strength function shown in Fig. 7; that is, the extra low-lying strength is responsible for an increase of the reaction cross section (and consequently of the Maxwellian-averaged reaction rate of astrophysical interest) by about a factor of three with respect to the predictions based on the HFB + QRPA calculation with BSk7 Skyrme force [15]. More specifically, the low-energy $E1$ strength originating from the PC contribution increases the cross section at 0.1 MeV (an energy of relevance for the r-process nucleosynthesis) by about 30% for ^{123}Sn(n, γ)^{124}Sn for the QTBA and by a factor of about two for QTBA-ws. For ^{131}Sn(n, γ)^{132}Sn these figures are even larger, and for ^{149}Sn(n, γ)^{150}Sn we obtained a similar effect for the QTBA-ws only. Thus, in this section we demonstrated the noticeable sensitivity of the radiative neutron capture cross section with respect to the model (QRPA, QTBA, or QTBA-ws) as well as the force used (SLy4 or BSk7).

B. Comparison with phenomenological models

The Lorentzian approach has been widely used for practical applications, although it suffers from shortcomings of various sorts. On the one hand, the location of the GDR maximum energy and width remains to be predicted from some underlying model for each nucleus. For many applications, these properties have often been obtained from a droplet-type model or from experimental systematics [20]. As shown in Fig. 3, these estimates may differ significantly from the predictions obtained from sounder microscopic models. In addition, the Lorentzian model tends to overestimate the $E1$ strength at energies below the neutron separation energy. Different parametrizations or functional forms (including, in particular, an energy- and temperature-dependent width) have been proposed (see, e.g., [20,68]) to reconcile experimental data in the photon or radiative neutron capture channels, but none of the proposed closed forms can nowadays explain the various trends observed at low energies. Besides, the Lorentzian approach cannot provide any predictions on the low-energy PDR; neither on its presence, nor on its characteristics. For this reason, it is of particular interest to analyze to what extent our predictions based on self-consistent microscopic models differ from those used in practical applications.

In Fig. 8 our results are compared with those obtained with the phenomenological generalized Lorentzian (GLO) strength function [68]. For the stable ^{124}Sn, the GLO cross section is rather similar to those obtained within the ETFFS approach. To be exact, this cross-section curve is just between the QTBA and QTBA-ws curves, although the strength functions can differ at low energies below the neutron separation energy (Fig. 7). However, for neutron-rich nuclei, such as ^{132}Sn and ^{150}Sn, the cross section obtained with the GLO strength on the one hand and both the QRPA and QTBA on the other hand differ, especially for ^{150}Sn. As shown in Sec. II, the main reason lies in the A dependence of the integral characteristics, but also in the existence of a low-lying strength predicted by the microscopic models. Note that the GLO parameters used here for ^{150}Sn correspond to the Reference Input Parameter Library (RIPL2)-recommended systematics (i.e., $E_0 = 14.81$ MeV, $\Gamma = 4.47$ MeV, and $\sigma_0 = 341.5$ mb), which strongly differ

from our microscopic predictions (see Fig. 3). Figure 7 also shows the spreading of the strength function down to the lowest energies (i.e., in the vicinity of the neutron separation energy), while the GLO model would only provide the tail of the GDR strength at these energies. These comparisons demonstrate the nonapplicability of the empirical systematics and the necessity to make use of self-consistent approaches for neutron-rich nuclei. (Regarding the comparisons of $M1$ resonances with the systematics used, see Ref. [69].)

IV. CONCLUSION

The electric dipole strength function has been estimated on the basis of the ETFFS(QTBA) model which simultaneously takes into account the (Q)RPA configurations, the more complex 1p1h $\otimes$ phonon or 2 quasiparticle $\otimes$ phonon configurations and the single-particle continuum. For the long chain of tin isotopes, the strength functions have been determined within our DTBA approach, which is a discretized self-consistent version of the ETFFS(QTBA). The QTBA strengths have been compared with the (Q)RPA ones which allowed us to study the contribution of the phonon coupling along the whole isotopic chain.

Our conclusions concerning the GDR and PDR properties clearly differ depending on the nuclear region considered, namely the $A < 132$ and $A > 132$ regions. More precisely:

(i) For neutron-rich $A > 132$ Sn isotopes, we find, both within QRPA and QTBA, a significant difference in the A dependence of the GDR mean energy on the standard phenomenological systematics. Our Eq. (3) gives new phenomenological systematics.

(ii) Although for all considered isotopes, the PC contribution to the GDR width is very important quantitatively, its contribution to nuclei in the $A > 132$ region is smaller than it is for the $A < 132$ nuclei.

(iii) The PC contribution to the PDR integral characteristics $\langle E \rangle$ and $\Sigma B(E1)$ summed over the 0–10 MeV interval is small for the neutron-rich isotopes.

(iv) The transition densities in most of the low-energy region are mainly of isoscalar nature both within the QRPA and QTBA approaches. The PC contribution to the transition densities also affects the transition densities, especially in stable nuclei. Globally, the isoscalar behavior is revealed on the energy interval considered here (1 MeV). It is not found that the transition density of all individual peaks in the low-energy region is of isoscalar nature. We note also that, for these reasons, the QRPA cannot explain quantitatively the isoscalar-isovector splitting of the PDR in the stable ^{140}Ce observed in the $(\alpha, \alpha'\gamma)$ reaction [60] (see Ref. [21] as well).

Such a different manifestation of PC for nuclei with $A < 132$ and $A > 132$ correlates very well with the neutron separation energy; namely, the differences are much smaller for neutron-rich nuclei than they are for $A < 132$ nuclei. Owing just to this fact, the low-energy parts of the strength functions in neutron-rich nuclei are rather similar within the QRPA and QTBA.

The radiative neutron capture cross sections for ^{124}Sn, ^{132}Sn, and ^{150}Sn were calculated with the QTBA and QRPA strength functions and shown to be sensitive to the predicted low-lying strength. Significant deviations from the phenomenological GLO approach [68] are also obtained for the strength functions and, consequently, for the neutron capture and photoabsorption cross sections for the very neutron-rich isotope ^{150}Sn. A direct comparison between the QTBA (including PC) and GLO cross sections shows that the neutron capture cross section on very neutron-rich nuclei may be increased by two orders of magnitude with respect to the traditional use of phenomenological models. Our results confirm the necessity to use self-consistent microscopic models when dealing with exotic nuclei. Therefore, nuclear data libraries should not recommend such phenomenological models in this case, but rather point toward newly developed microscopic large-scale calculations.

In our calculations, phonon coupling, which has been included, in addition to the standard QRPA, is a necessary ingredient to describe the electric GDR and PDR properly. Nevertheless, it is necessary to use some renormalization procedures (either by adjusting some interaction parameters or by applying the subtraction method) to obtain the correct value of the spurious state energy. In addition, the approach still needs to include the self-consistency at the level of complex configurations. Therefore, further developments are needed (see also [21], where some unsolved issues in the PDR physics are discussed).

ACKNOWLEDGMENTS

We thank Professor J. Speth for valuable discussions and Dr. N. A. Lyutorovich for the RPA single-particle continuum results shown in Fig. 2 for magic nuclei ^{132}Sn and ^{176}Sn. The work was partly supported by the DFG Grant No. 436RUS113/994/0-1 and RFBR Grant No. 09-02-91352NNIOa.

[1] V. G. Soloviev, *Theory of Atomic Nuclei: Quasiparticles and Phonons* (Institute of Physics, Bristol and Philadelphia, 1992).
[2] G. Colo, N. Van Giai, P. F. Bortignon, and R. A. Broglia, Phys. Rev. C **50**, 1496 (1994).
[3] S. Kamerdzhiev, J. Speth, and G. Tertychny, Phys. Rep. **393**, 1 (2004).
[4] V. Tselyaev, Phys. Rev. C **75**, 024306 (2007).
[5] N. Tsoneva and H. Lenske, Phys. Rev. C **77**, 024321 (2008).
[6] D. Sarchi, P. F. Bortignon, and G. Colo, Phys. Lett. B **601**, 27 (2004).
[7] E. Litvinova, P. Ring, and V. Tselyaev, Phys. Rev. C **78**, 014312 (2008).
[8] A. Avdeenkov, F. Gruemmer, Phys. Lett. B **653**, 196 (2007).
[9] S. Kamerdzhiev, Bul. Rus. Acad. Sci. Phys. **61**, 152 (1997).
[10] S. Kamerdzhiev and E. Litvinova, Phys. At. Nucl. **64**, 627 (2001).

[11] S. Kamerdzhiev, R. Liotta, E. Litvinova, and V. Tselyaev, Phys. Rev. C **58**, 172 (1998).
[12] E. Litvinova and V. Tselyaev, Phys. Rev. C **75**, 054318 (2007).
[13] N. Paar, D. Vretenar, E. Khan, and G. Colo, Rep. Prog. Phys. **70**, 691 (2007).
[14] S. Goriely and E. Khan, Nucl. Phys. A **706**, 217 (2002).
[15] S. Goriely, E. Khan, and M. Samyn, Nucl. Phys. A **739**, 331 (2004).
[16] H. Sagawa and H. Esbensen, Nucl. Phys. A **693**, 448 (2001).
[17] L. Capelli, G. Colo, and J. Li, Phys. Rev. C **79**, 054329 (2009).
[18] U. Kneisl, N. Pietralla, and A. Zilges, J. Phys. G **32**, R217 (2006).
[19] S. Volz, N. Tsoneva, Nucl. Phys. A **779**, 1 (2006).
[20] T. Belgya *et al.*, *Handbook for Calculations of Nuclear Reaction Data, RIPL-2*, IAEA-Tecdoc-1506 (2006).
[21] A. V. Avdeenkov and S. P. Kamerdzhiev, Phys. At. Nucl. **72**, 1332 (2009).
[22] S. Krewald and J. Speth, Int. J. Mod. Phys. E **18**, 1425 (2009).
[23] S. Goriely, Phys. Lett. B **436**, 10 (1998).
[24] R. Capote *et al.*, Nucl. Data Sheets **110**, 3107 (2009).
[25] O. Wieland, A. Bracco, and F. Camera, Phys. Rev. Lett. **102**, 092502 (2009).
[26] Y. Suzuki, K. Ikeda, and H. Sato, Prog. Theor. Phys. **83**, 180 (1990).
[27] G. Tertychny, V. Tselyaev, Phys. Lett. B **647**, 104 (2007).
[28] A. Avdeenkov, S. Goriely, S. Kamerdzhiev, and G. Tertychny, AIP Conf. Proc. **1090**, 149 (2009).
[29] G. Colo and P. F. Bortignon, Nucl. Phys. A **696**, 427 (2001).
[30] S. P. Kamerdzhiev and E. V. Litvinova, Phys. At. Nucl. **67**, 183 (2004).
[31] R.-D. Herzberg *et al.*, Phys. Lett. B **390**, 49 (1997).
[32] K. Govaert *et al.*, Phys. Rev. C **57**, 2229 (1998).
[33] A. V. Avdeenkov, S. Goriely, and S. P. Kamerdzhiev, Phys. At. Nucl. **73**, 1119 (2010).
[34] N. Lyutorovich *et al.*, EPJA **37**, 381 (2008).
[35] M. Bender, G. F. Bertsch, and P.-H. Heenen, Phys. Rev. C **73**, 034322 (2006).
[36] M. Kortelainen, J. Dobaczewski, K. Mizuyama, and J. Toivanen, Phys. Rev. C **77**, 064307 (2008).
[37] E. Chabanat, P. Bonche, P. Haensel, J. Meyer, and R. Schaeffer, Nucl. Phys. A **635**, 231 (1998).
[38] J. Terasaki, J. Engel, Phys. Rev. C **71**, 034310 (2005).
[39] K. Bennaceur and J. Dobaczewski, Comput. Phys. Commun. **168**, 96 (2005).
[40] S. O. Backman, A. D. Jackson, and J. Speth, Phys. Lett. B **56** 209 (1975).
[41] S. Krewald, V. Klempt, J. Speth, and A. Faessler, Nucl. Phys. A **281**, 166 (1977).
[42] S. Shlomo and G. Bertsch, Nucl. Phys. A **243**, 507 (1975).
[43] E. E. Saperstein, A. V. Tolokonnikov, and S. A. Fayans, Preprint **IAE 2571** (Russian), Moscow (1975).
[44] B. K. Agrawal, S. Shlomo, and A. I. Sanzhur, Phys. Rev. C **67**, 034314 (2003).
[45] S. Kamerdzhiev, J. Speth, G. Tertychny, and V. Tselyaev, Nucl. Phys. A **555**, 90 (1993).
[46] V. I. Tselyaev, Bull. Rus. Acad. Sci. Phys. **64**, 434 (2000).
[47] S. P. Kamerdzhiev, Sov. J. Nucl. Phys. **38**, 188 (1983).
[48] D. Pena Arteaga, E. Khan, and P. Ring, Phys. Rev. C **79**, 034311 (2009).
[49] A. Adrich, A. Klimkiewicz, Phys. Rev. Lett. **95**, 132501 (2005).
[50] M. Samyn, S. Goriely, P.-H. Heenen, J. M. Pearson, and F. Tondeur, Nucl. Phys. A **700**, 142 (2002).
[51] J. Bartel, P. Quentin, M. Brack, C. Guet, and H.-B. Hakansson, Nucl. Phys. A **386**, 79 (1982).
[52] P. Ring and P. Schuck, *The Nuclear Many-Body Problem*, (Springer, Berlin, 1980).
[53] V. Tselyaev, J. Speth, F. Gruemmer, S. Krewald, A. Avdeenkov, E. Litvinova, and G. Tertychny, Phys. Rev. C **75**, 014315 (2007).
[54] E. Litvinova, P. Ring, V. Tselyaev, and K. Langanke, Phys. Rev. C **79**, 054312 (2009).
[55] B. Ozel, J. Enders, Nucl. Phys. A **788**, 385 (2007).
[56] P. Van Isacker, M. A. Nagarajan, and D. D. Warner, Phys. Rev. C **45**, R13 (1992).
[57] A. Klimkiewicz, P. Adrich, Nucl. Phys. A **788**, 145c (2007).
[58] E. G. Lanza, F. Catara, Phys. Rev. C **79**, 054615 (2009).
[59] J. Terasaki and J. Engel, Phys. Rev. C **74**, 044301 (2006).
[60] N. Paar, Y. F. Niu, D. Vretenar, and J. Meng, Phys. Rev. Lett. **103**, 032502 (2009).
[61] M. Arnould, S. Goriely, and T. Takahashi, Phys. Rep. **450**, 97 (2007).
[62] M. Arnould and S. Goriely, Phys. Rep. **384**, 1 (2003).
[63] S. Goriely, S. Hilaire, and A. J. Konig, Astron. Astrophys. **487**, 767 (2008).
[64] EXFORlibrary: [http://www-nds.iaea.or.at/exfor].
[65] E. Litvinova, H. P. Loens, K. Langanke, G. Martinez-Pinedo, T. Rauscher, P. Ring, F.-K. Thielemann, and V. Tselyaev, Nucl. Phys. A **823**, 26 (2009).
[66] T. Rauscher, Phys. Rev. C **78**, 032801 (2008).
[67] A. Avdeenkov, S. Goriely, and S. Kamerdzhiev, *Proc. Int. Conf. on Nuclear Data* (26-30.04.2010, Korea, to be published), arXiv:1103.2630v1.
[68] J. Kopecky and M. Uhl, Phys. Rev. C **41**, 1941 (1990).
[69] S. P. Kamerdzhiev and S. F. Kovalev, Phys. At. Nucl. **69**, 418 (2006).